

An interferometric theory of source-receiver scattering and imaging

David Halliday¹ and Andrew Curtis²

ABSTRACT

It is known that there is a link between the theory of seismic interferometry and theories of seismic imaging and inversion. However, although this has been discussed in several studies, there are few where any explicit links have been derived. We use reciprocity theorems for scattering media to derive a new form of seismic interferometry that describes the scattered wavefield between a source and a receiver in an acoustic medium, using both sources and receivers on two enclosing boundaries. This form of seismic interferometry is equivalent to a generalized imaging condition (IC) that combines the full wavefield inside any finite-sized subregion of the medium of interest. By using the Born (single-scattering) approximation, this generalized IC reduces to the method of imaging by double-focusing originally derived by Michael Oristaglio in 1989. Thus an explicit link is made between seismic interferometry, new generalized full-wavefield ICs, and existing single-scattering imaging methods.

INTRODUCTION

Generally, seismic interferometry refers to the recovery of the wavefield propagating between two receiver locations (as if one receiver was replaced by a source) by crosscorrelating the wavefields observed at each receiver location due to an enclosing boundary of energy sources (Wapenaar, 2003, 2004; van Manen et al., 2005, 2006; Wapenaar and Fokkema, 2006). The method is not restricted to seismic wavefields; for example, studies have been carried out for acoustic media (Derode et al., 2003; van Manen et al., 2005, 2006) and electromagnetic media (Slob and Wapenaar, 2007; Slob et al., 2007), and a unified approach allows application to other wave phenomena such as seismo-electric wave propagation and diffusive wavefields (Wapenaar et al., 2006; Snieder et al., 2007; Vasconcelos, 2008). More recent advances have shown that the method can be applied using cross-convolution (Slob et al., 2007; Wapenaar, 2007;

Halliday and Curtis, 2009b) or deconvolution (Vasconcelos and Snieder 2008a, b; Wapenaar et al., 2008b) in place of the crosscorrelation operator. Further, Curtis et al. (2009) show that, by using reciprocity, the role of source and receiver can be reversed; i.e., the wavefield propagating between two sources can be recovered using recordings of those sources on an enclosing boundary.

Although many applications of the method have been proposed and tested (see Curtis et al., 2006 and Wapenaar et al., 2008a for more detailed applications), in this paper we expand upon recent advances made by Curtis and Halliday (2010b), who showed that it is possible to derive new representation theorems and interferometric relations for source-receiver (as opposed to inter-source or inter-receiver) wavefields. Whereas “conventional” interferometry uses a single boundary surface of sources to estimate the wavefield between two receiver locations in the interior of that surface, source-receiver interferometry uses a boundary of sources *and* a boundary of receivers to construct the wavefield between a source location and a receiver location.

Using an approach similar to that of Curtis and Halliday (2010b), we derive a new form of interferometric integral that describes the recovery of *scattered* waves propagating between a real source and a real receiver. This is done using the scattering reciprocity theorems of Vasconcelos et al. (2009a). We then show that it is possible to create an explicit link between this form of seismic interferometry and inverse-scattering seismic imaging theory (also see Vasconcelos et al., 2009b). More specifically, by using a single-scattering Born approximation, we present an alternative derivation of Oristaglio’s (1989) inverse-scattering formula, which we derive directly from source-receiver interferometry. This formula is now recognized as a fundamental basis for many modern imaging algorithms. For example, we can recognize more modern double-focusing imaging conditions to be similar to that derived by Oristaglio (Berkhout, 1997; Schuster and Hu, 2000), and we can also recognize relations between Oristaglio’s formula and those formulae used in creating extended images using image-domain interferometry (e.g., Vasconcelos et al., 2009b). This link is only made possible by using the scattering form of source-receiver interferometry that we derive here. This

Manuscript received by the Editor 19 October 2009; revised manuscript received 14 April 2010; published online 21 October 2010.

¹Schlumberger Cambridge Research, Cambridge, U. K. E-mail: dhalliday@slb.com.

²University of Edinburgh, School of GeoSciences, Edinburgh, U. K. E-mail: andrew.curtis@ed.ac.uk.

© 2010 Society of Exploration Geophysicists. All rights reserved.

may also allow new approaches for scattered ground-roll removal to be developed (e.g., see [Halliday et al., 2010](#)).

The link between seismic interferometry and imaging has previously been discussed by [Wapenaar \(2007\)](#), [Thorbecke and Wapenaar \(2007\)](#), and [Vasconcelos \(2008\)](#). In [Thorbecke and Wapenaar \(2007\)](#), the connection between the work of [Oristaglio](#) and seismic interferometry is discussed, but the link could not be made explicit. This is because those authors discussed preexisting interferometric integrals that consider only sources on a surrounding surface. The theory of interferometry in [Curtis and Halliday \(2010b\)](#) includes both sources and receivers on either the same, or on different surfaces, and, hence, so does our new scattering theory presented herein. This is more representative of imaging applications, for example, in seismic imaging where sources and receivers are located at different positions at the surface of the Earth and/or in subsurface wells. This is the reason that this is the first time that a link between interferometry and existing inverse-scattering imaging methods could be derived explicitly.

In the first part of this paper, we use two scattering reciprocity theorems of the correlation-type to derive a source-receiver interferometric relation for scattered waves in acoustic media. This new relation is an example of one of many different relations that can be derived using different source and receiver configurations ([Curtis and Halliday, 2010b](#)). In the second part of this paper we show how the source-receiver interferometric relation can be used to derive the inverse-scattering formula of [Oristaglio \(1989\)](#). This creates the explicit link between the new source-receiver relationship and seismic imaging. Finally, we discuss the implications of this work.

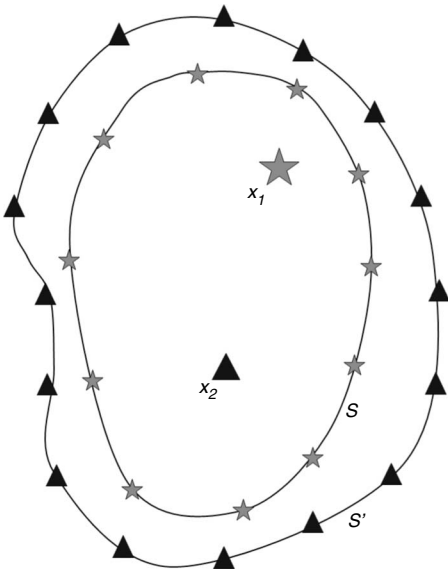


Figure 1. Configuration for source-receiver interferometry using two correlational integrals. Source-receiver interferometry estimates the scattered wavefield between a source (\mathbf{x}_1) and receivers (\mathbf{x}_2) using a boundary of sources (S) and a boundary of receivers (S'). S and S' are closed lines in two dimensions, surfaces in three dimensions.

SOURCE-RECEIVER INTERFEROMETRY FOR SCATTERED WAVEFIELDS

[Curtis and Halliday \(2010b\)](#) showed that the combination of two representation theorems (either of the correlation-type or the convolution-type) allows for a new form of interferometric integral. These integrals describe the recovery of waves propagating between a single source and a receiver by using only wavefields propagating both from and to surrounding boundaries of sources and receivers (Figure 1).

We now extend this derivation to scattered wavefields using two correlation-type scattering reciprocity theorems. Typically, interferometric relations are derived using a single reciprocity theorem with two independent wavefield states ([Fokkema and van den Berg, 1993](#); [Wapenaar and Fokkema, 2006](#)). In the following we use two reciprocity theorems with three independent wavefield states. Later this allows us to combine the two integral equations derived from equations 1 and 2 (below), resulting in the source-receiver form of interferometry that involves two surface integrals. We therefore begin with the following two reciprocity relations for perturbed media from [Vasconcelos et al. \(2009a\)](#). These describe relationships among the scattered wavefield components caused by perturbations to the medium, the wavefield in the unperturbed or background medium, and the full wavefield in the perturbed medium:

$$\int_V p_A^S q_B^{0*} dV - \int_V j\omega(\kappa_0 - \kappa) p_A p_B^{0*} dV = \int_S \{p_A^S v_{i,B}^{0*} + v_{i,A}^S p_B^{0*}\} n_i dS, \quad (1)$$

$$\int_{V'} p_C^S q_A^{0*} dV' - \int_{V'} j\omega(\kappa'_0 - \kappa') p_C p_A^{0*} dV' = \int_{S'} \{p_C^S v_{i',A}^{0*} + v_{i',C}^S p_A^{0*}\} n_{i'} dS', \quad (2)$$

where, A , B , and C represent independent wavefield states (e.g., the wavefields that arise with two different boundary or initial conditions, possibly with two different sets of medium properties). Then p_A is the acoustic pressure in state A , q_A is a source distribution in state A in terms of volume injection-rate density, $v_{i,A}$ is the i th component of particle velocity in state A , and similarly for states B and C . The asterisk (*) denotes complex conjugation, j represents the square root of -1 , ω is the angular frequency, $\kappa_0 - \kappa$ is the perturbation to the compressibility, and n_i and $n_{i'}$ are the outward normals to the surfaces S' and S , respectively. Superscript S indicates the scattered field, superscript 0 indicates the field in the background medium, and no superscript indicates the full wavefield. We have assumed there are no sources of the unidirectional point-force type (this would require extra volume integral terms), and all expressions are formulated in the frequency domain. Surface S bounding volume V need not be the same as surface S' bounding volume V' (Figure 1).

Rather than derive new representation theorems as in [Curtis and Halliday \(2010b\)](#), we omit this intermediate step and immediately define the quantities required by equations 1 and 2 for three Green's states:

State A:

$$q_A^0(\mathbf{x}) = \delta(\mathbf{x} - \mathbf{x}_1), \quad p_A(\mathbf{x}) = G(\mathbf{x}, \mathbf{x}_1), \quad p_A^S(\mathbf{x}) = G_S(\mathbf{x}, \mathbf{x}_1),$$

$$v_{i,A}^S(\mathbf{x}) = \frac{-1}{j\omega\rho} \partial_i G_S(\mathbf{x}, \mathbf{x}_1), \quad p_A^0(\mathbf{x}) = G_0(\mathbf{x}, \mathbf{x}_1), \quad (3)$$

$$v_{i,A}^0(\mathbf{x}) = \frac{-1}{j\omega\rho} \partial_i G_0(\mathbf{x}, \mathbf{x}_1).$$

State B:

$$q_B^0(\mathbf{x}) = \delta(\mathbf{x} - \mathbf{x}_2), \quad p_B^0(\mathbf{x}) = G_0(\mathbf{x}, \mathbf{x}_2), \quad (4)$$

$$v_{i,B}^0(\mathbf{x}) = \frac{-1}{j\omega\rho} \partial_i G_0(\mathbf{x}, \mathbf{x}_2).$$

State C:

$$p_C^S(\mathbf{x}') = G_S(\mathbf{x}', \mathbf{x}), \quad v_{i',C}^S(\mathbf{x}') = \frac{-1}{j\omega\rho} \partial_{i'} G_S(\mathbf{x}', \mathbf{x}). \quad (5)$$

Here $G(\mathbf{x}, \mathbf{x}_1)$ is the full Green's function between a source at \mathbf{x}_1 and a receiver at \mathbf{x} , and $G_0(\mathbf{x}, \mathbf{x}_1)$ and $G_S(\mathbf{x}, \mathbf{x}_1)$ are the equivalent Green's function in the unperturbed background medium, and the Green's function representing the scattered wavefield, respectively. $p_A(\mathbf{x}')$ is the acoustic pressure at \mathbf{x}' in state A, $v_{i,A}(\mathbf{x})$ is the i th component of particle velocity at \mathbf{x} in state A (and similarly for states B and C), and superscripts 0 and S indicate the quantities corresponding to the wavefield in the background medium, and the scattered wavefield, respectively, and no superscript indicates the full wavefield. ∂_i is the spatial derivative in the i -direction, ρ is the density and $p(\mathbf{x}) = p^0(\mathbf{x}) + p^S(\mathbf{x})$. Using these three states allow us to write equations 1 and 2 as follows (see Vasconcelos et al., 2009a):

$$G_S(\mathbf{x}_2, \mathbf{x}_1) = j\omega \int_V (\kappa_0 - \kappa) G(\mathbf{x}, \mathbf{x}_1) G_0^*(\mathbf{x}, \mathbf{x}_2) dV$$

$$+ \frac{-1}{j\omega\rho} \int_S \{n_i \partial_i G_S(\mathbf{x}, \mathbf{x}_1) G_0^*(\mathbf{x}, \mathbf{x}_2)$$

$$- G_S(\mathbf{x}, \mathbf{x}_1) n_i \partial_i G_0^*(\mathbf{x}, \mathbf{x}_2)\} dS, \quad (6)$$

and

$$G_S(\mathbf{x}_1, \mathbf{x}) = j\omega \int_{V'} (\kappa'_0 - \kappa') G(\mathbf{x}', \mathbf{x}) G_0^*(\mathbf{x}', \mathbf{x}_1) dV'$$

$$+ \frac{-1}{j\omega\rho} \int_{S'} \{n_{i'} \partial_{i'} G_S(\mathbf{x}', \mathbf{x}) G_0^*(\mathbf{x}', \mathbf{x}_1)$$

$$- G_S(\mathbf{x}', \mathbf{x}) n_{i'} \partial_{i'} G_0^*(\mathbf{x}', \mathbf{x}_1)\} dS'. \quad (7)$$

Note that in equations 6 and 7, and all following equations, where a derivative operator such as ∂_i , immediately precedes a Green's function, it is to be understood that the derivative operator is acting on that Green's function. Where the derivative operator precedes bracketed terms, it is to be understood that the derivative operator acts after evaluation of the terms within the bracket. We now consider the configuration illustrated in Figure 1: there is a receiver at \mathbf{x}_2 , a source at \mathbf{x}_1 , the boundary S is populated by sources, the boundary S' is populated by receivers, and \mathbf{x}_2 and \mathbf{x}_1 are inside both surfaces S and S' .

This configuration is possible due to source-receiver reciprocity (i.e., source and receiver positions can be freely interchanged). In this configuration $G_S(\mathbf{x}, \mathbf{x}_1)$ is the scattered Green's function between two sources, and using source-receiver reciprocity, such that $G_S(\mathbf{x}, \mathbf{x}_1) = G_S(\mathbf{x}_1, \mathbf{x})$, this is equal to the left-hand side of equation 7. This is not a measured quantity, so we substitute equation 7, which only contains measured (i.e., source-receiver) quantities, into equation 6, resulting in

$$G_S(\mathbf{x}_2, \mathbf{x}_1) = j\omega \int_V (\kappa_0 - \kappa) G(\mathbf{x}, \mathbf{x}_1) G_0^*(\mathbf{x}, \mathbf{x}_2) dV$$

$$+ \frac{-1}{j\omega\rho} \int_S \left\{ n_i \partial_i \left[j\omega \int_{V'} (\kappa'_0 - \kappa') G(\mathbf{x}', \mathbf{x}) \right. \right.$$

$$\times G_0^*(\mathbf{x}', \mathbf{x}_1) dV' \left. \right\} G_0^*(\mathbf{x}, \mathbf{x}_2)$$

$$- \left[j\omega \int_{V'} (\kappa'_0 - \kappa') G(\mathbf{x}', \mathbf{x}) \right.$$

$$\times G_0^*(\mathbf{x}', \mathbf{x}_1) dV' \left. \right\} n_i \partial_i G_0^*(\mathbf{x}, \mathbf{x}_2) \left. \right\} dS$$

$$+ \frac{-1}{j\omega\rho} \int_S \left\{ n_i \partial_i \left[\frac{-1}{j\omega\rho} \int_{S'} \{n_{i'} \partial_{i'} G_S(\mathbf{x}', \mathbf{x}) \right. \right.$$

$$\times G_0^*(\mathbf{x}', \mathbf{x}_1) - G_S(\mathbf{x}', \mathbf{x})$$

$$\times n_{i'} \partial_{i'} G_0^*(\mathbf{x}', \mathbf{x}_1)\} dS' \left. \right\} G_0^*(\mathbf{x}, \mathbf{x}_2)$$

$$- \left[\frac{-1}{j\omega\rho} \int_{S'} \{n_{i'} \partial_{i'} G_S(\mathbf{x}', \mathbf{x}) G_0^*(\mathbf{x}', \mathbf{x}_1) \right.$$

$$- G_S(\mathbf{x}', \mathbf{x}) n_{i'} \partial_{i'} G_0^*(\mathbf{x}', \mathbf{x}_1)\} dS' \left. \right\}$$

$$\times n_i \partial_i G_0^*(\mathbf{x}, \mathbf{x}_2) \left. \right\} dS. \quad (8)$$

Equation 8 describes the reconstruction of the scattered waves propagating between a source at \mathbf{x}_1 and a receiver at \mathbf{x}_2 using only energy that has propagated from and to the surrounding boundaries of sources and receivers. The first volume integral contributes to the perturbed wavefield due to perturbations within the volume V , and the combination of surface and volume integrals (second term) contributes to the perturbed wavefield due to perturbations within the volume V' (similar volume integrals are discussed by Vasconcelos et al., 2009a). The double surface integral in the last term describes a first step in determining the scattered wavefield between a source at \mathbf{x}_1 and a receiver at \mathbf{x}_2 , where the scattered waves between \mathbf{x} and \mathbf{x}_1 are reconstructed by means of the inner integral over S' . In a second step the scattered waves between \mathbf{x}_2 and \mathbf{x}_1 are reconstructed by means of the outer integral over S . Note that when we describe these as “inner” and “outer” integrals, we are referring to their position in equation 8, rather than their physical position in Figure 1. Equation 8 is equivalent to equation 1 in Vasconcelos et al. (2009b), but includes

the wavefield extrapolation defined by equation 7 and the associated volume terms.

We isolate the quantities dependant on \mathbf{x} in the second term of equation 8:

$$\frac{-1}{j\omega\rho} \int_S \{n_i \partial_i G(\mathbf{x}', \mathbf{x}) G_0^*(\mathbf{x}, \mathbf{x}_2) - G(\mathbf{x}', \mathbf{x}) n_i \partial_i G_0^*(\mathbf{x}, \mathbf{x}_2)\} dS. \quad (9)$$

This can then be split into two surface integrals by substituting $G(\mathbf{x}', \mathbf{x}) = G_0(\mathbf{x}', \mathbf{x}) + G_S(\mathbf{x}', \mathbf{x})$,

$$\begin{aligned} & \frac{-1}{j\omega\rho} \int_S \{n_i \partial_i G_0(\mathbf{x}', \mathbf{x}) G_0^*(\mathbf{x}, \mathbf{x}_2) - G_0(\mathbf{x}', \mathbf{x}) n_i \partial_i G_0^*(\mathbf{x}, \mathbf{x}_2)\} dS \\ & + \frac{-1}{j\omega\rho} \int_S \{n_i \partial_i G_S(\mathbf{x}', \mathbf{x}) G_0^*(\mathbf{x}, \mathbf{x}_2) \\ & - G_S(\mathbf{x}', \mathbf{x}) n_i \partial_i G_0^*(\mathbf{x}, \mathbf{x}_2)\} dS \\ & = G_0^*(\mathbf{x}', \mathbf{x}_2) + G_0(\mathbf{x}', \mathbf{x}_2) + G_S(\mathbf{x}_2, \mathbf{x}') \\ & - j\omega \int_V (\kappa_0 - \kappa) G(\mathbf{x}, \mathbf{x}') G_0^*(\mathbf{x}, \mathbf{x}_2) dV. \end{aligned} \quad (10)$$

The terms $G_0^*(\mathbf{x}', \mathbf{x}_2)$ and $G_0(\mathbf{x}', \mathbf{x}_2)$ arise from the first surface integral on the left-hand side of equation 10, and the other two terms on the right-hand side arise from the second surface integral on the left-hand side (see Vasconcelos et al., 2009a, equation 14). This involves the crosscorrelation of waves in the background medium with the full wavefield. The second integral on the left-hand side of equation 10 has the form of the back-propagation operator that is used in seismic imaging (e.g., Esmersoy and Oristaglio, 1988; Wang and Oristaglio, 1998; Thorbecke and Wapenaar, 2007). In equation 10, rather than crosscorrelating just the scattered wavefield G_S , the full field G

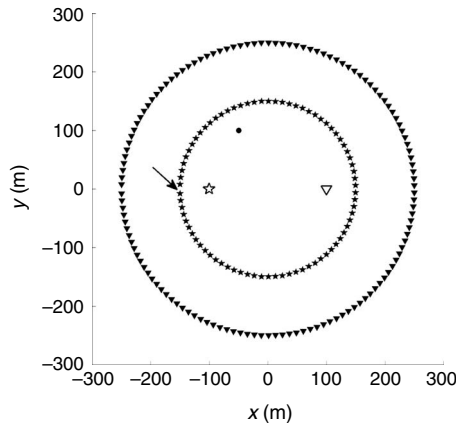


Figure 2. Geometry for the single-scatterer example. Black triangles indicate the receiver boundary, and black stars indicate the source boundary. Source-receiver interferometry is used to estimate the scattered wave (and associated terms) between the open star and the open triangle. The scatterer is indicated by the black dot. This example is in two dimensions. Compare the geometry here with that sketched in Figure 1. The background wave propagation velocity is 750 m/s. The distance between the source (open star) and the scatterer is 110 m, and the distance between the scatterer and the receiver (open triangle) is 180 m.

$= G_0 + G_S$ is used. Using only the scattered field causes the background Green's functions to drop out of the right-hand side of equation 10; hence, the scattered term and volume integral on the right-hand side are the back-propagated wavefield used in seismic imaging.

NUMERICAL EXAMPLE

We now illustrate scattered wave estimation using equation 8. To simplify the application of this equation we use the same approximation as is often invoked in more conventional applications of interferometry (e.g., Wapenaar and Fokkema, 2006) and assume that the outer boundary S' has a large radius; hence, in equation 8 we use the Sommerfield radiation conditions ($\mp jkG = n_i \partial_i G$ with $-$ indicating outgoing waves and $+$ indicating incoming waves at the boundary; these conditions hold if waves travel perpendicularly to the boundaries). We also assume that the medium is smooth at and around this boundary and that the medium is homogeneous outside of this boundary (Wapenaar and Fokkema, 2006). We also move the terms containing volume integrals to the left-hand side because their interpretation is quite distinct from that of the surface integral. These operations and assumptions give equation 11:

$$\begin{aligned} & G_S(\mathbf{x}_2, \mathbf{x}_1) - j\omega \int_V (\kappa_0 - \kappa) G(\mathbf{x}, \mathbf{x}_1) G_0^*(\mathbf{x}, \mathbf{x}_2) dV \\ & - \frac{-1}{j\omega\rho} \int_S \left\{ n_i \partial_i \left[j\omega \int_{V'} (\kappa'_0 - \kappa') G(\mathbf{x}', \mathbf{x}) \right. \right. \\ & \left. \left. \times G_0^*(\mathbf{x}', \mathbf{x}_1) dV' \right] G_0^*(\mathbf{x}, \mathbf{x}_2) \right. \\ & - \left[j\omega \int_{V'} (\kappa'_0 - \kappa') G(\mathbf{x}', \mathbf{x}) \right. \\ & \left. \times G_0^*(\mathbf{x}', \mathbf{x}_1) dV' \right] n_i \partial_i G_0^*(\mathbf{x}, \mathbf{x}_2) \left. \right\} dS \\ & \approx \frac{-1}{j\omega\rho} \int_S \left\{ n_i \partial_i \left[\frac{2}{c\rho} \int_{S'} G_S(\mathbf{x}', \mathbf{x}) G_0^*(\mathbf{x}', \mathbf{x}_1) dS' \right] G_0^*(\mathbf{x}, \mathbf{x}_2) \right. \\ & \left. - \left[\frac{2}{c\rho} \int_{S'} G_S(\mathbf{x}', \mathbf{x}) G_0^*(\mathbf{x}', \mathbf{x}_1) dS' \right] n_i \partial_i G_0^*(\mathbf{x}, \mathbf{x}_2) \right\} dS. \end{aligned} \quad (11)$$

Here, c is the local wave propagation velocity at the boundary. Thus, due to the far-field conditions we require only pressure recordings on the outer boundary. The geometry for this example is shown in Figure 2. We use circular boundaries of sources (black stars) and receivers (black triangles), to estimate the wave scattered by a single point scatterer (black dot) between a source (open star) and a receiver (open triangle). We model wavefields using a deterministic variant of Foldy's method (Groenenboom and Snieder, 1995; van Manen et al., 2006; Curtis and Halliday, 2010a). This modeling method ensures that energy is conserved between the incident and scattered wave and hence is consistent with the optical theorem, which is important when analyzing seismic interferometry using modeled wavefields (Snieder et al., 2008; Halliday and Curtis, 2009a, b).

In Figure 3a we show the result of the inner integrand on the right-hand side of equation 11 for all boundary receivers \mathbf{x}' and one pair of sources at \mathbf{x} (indicated by an arrow in Figure 2) and \mathbf{x}_1 , respectively. In Figure 3b we show the result of the integral — the sum of the signals in Figure 3a over the set of all boundary receivers. There are two arrivals in this plot: one corresponds to the inter-receiver scattered wave (arriving at about 0.45 s), and the other corresponds to the volume integral over V' on the left-hand side of equation 11 (arriving at about 0.15 s). Figure 4a shows the result of the outer integrand on the right-hand side of equation 11; this is computed after the inner integral has been computed. The result of computing this outer integral is shown in Figure 4b (solid line). We evaluate the left-hand side of equation 11 and plot this for comparison (dotted line). Note that despite the far-field approximations used in equation 11 the dotted line matches the solid line.

The result of the integral is the scattered surface wave plus several nonphysical events (events that do not correspond to any event in the true source-receiver response). Such events have been identified before in seismic interferometry, and steps can be taken to mitigate for their effect. For example, Curtis and Halliday (2010a) propose to estimate and adaptively subtract estimates of the nonphysical events, and Vasconcelos et al. (2009a) propose to use a limited integration boundary to remove the effects of these events.

Finally, we show the right-hand side of equation 11 (solid line) plotted together with the first term on the left-hand side (the exact scattered wave: dotted line, Figure 5a), together with the second term on the left-hand side (the volume integral over V : dotted line, Figure 5b), and together with the third term on the left-hand side (the combination of surface integral and volume integral: dotted line, Figure 5c). These extra terms complicate the result of equation 11 and would often be treated as nonphysical arrivals in seismic interferometry. Note that in Figure 5c the third term on the left-hand side of equation 11 appears to give a nonphysical event (at about 0.08 s) and also the time-reverse of the exact scattered wave shown in Figure 5a (at about -0.4 s). We now show that all of these terms contain important information in applications of integrals such as equation 8 to seismic imaging. (The significance of such volume terms was identified by Vasconcelos et al. (2009b) who postulated that the volume terms would be useful when dealing with sharp boundaries in background velocity models). To do this we present an alternative

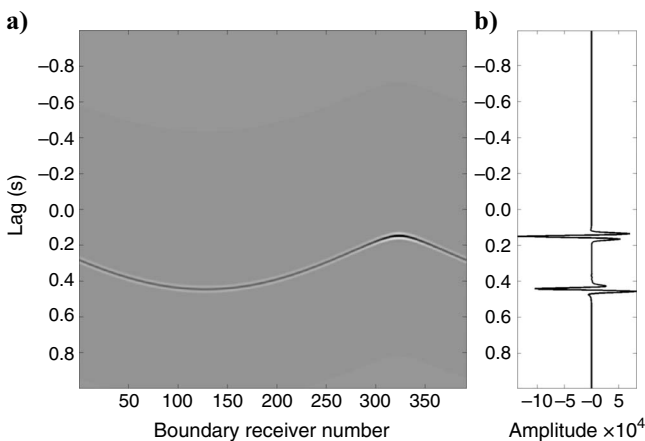


Figure 3. (a) The inner integrand on the right-hand side of equation 11, for one source pair (\mathbf{x} and \mathbf{x}_1). (b) The solution of the inner integral [summation of (a) over boundary receiver number].

derivation of Oristaglio's (1989) imaging condition. This acts to further provide understanding of how such imaging theories can be applied when surfaces of sources S and of receivers S' are not coincident. Also, because the far-field conditions deployed to obtain equation 11 are often invoked in order to represent interferometry using an outer boundary of passive noise sources, this will show how both energy from passive noise and active sources can be combined to create a subsurface image.

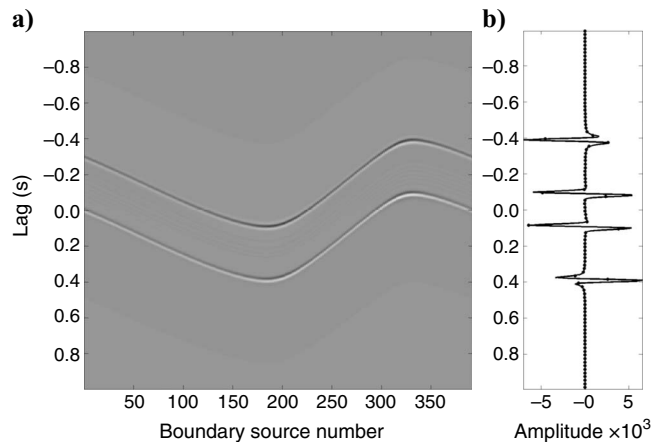


Figure 4. (a) The outer integrand on the right-hand side of equation 11 after the solution of the inner integral as illustrated in Figure 3b. (b) The solution of the integral [summation of (a) over boundary source number]. The left-hand side of equation 10 is plotted for reference (dotted line).

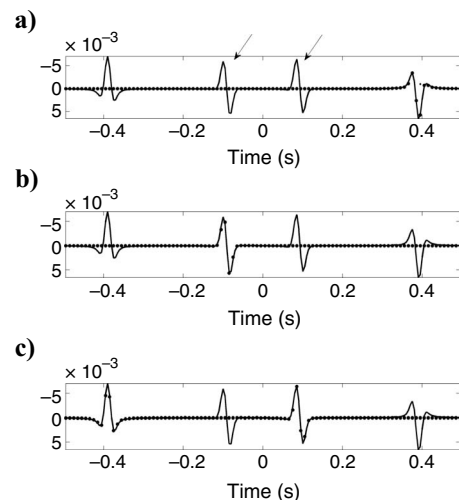


Figure 5. Result of equation 10 (solid line) plotted with (a) the directly modeled scattered wavefield (dotted line), (b) the solution of the volume integral over V from the left-hand side of equation 11, and (c) the result of the volume integral over V' and the surface integral over S . The arrows in (a) indicate the events interpreted as nonphysical arrivals. The arrival at 0.4 s is clearly interpreted as the scattered wave, and the arrival at -0.4 s is interpreted as the time reverse of this scattered wave.

The link with Oristaglio's imaging condition

Within the first-order Born approximation (assuming there are no significant multiply scattered waves), Oristaglio (1989) derived a formula for the scattering potential, $f(\mathbf{x}_1)$ at location \mathbf{x}_1 as

$$\begin{aligned}
 f(\mathbf{x}_1) = & \frac{4}{jc_0} \int_{-\infty}^{\infty} d\omega (-j\omega) \frac{\partial}{\partial \omega} \frac{1}{\omega^2} \\
 & \times \int_S \left\{ n_i \partial_i \left[\int_{S'} \{ G_0^*(\mathbf{x}_1, \mathbf{x}') n_{i'} \partial_{i'} G_S(\mathbf{x}', \mathbf{x}) \right. \right. \\
 & \left. \left. - G_S(\mathbf{x}', \mathbf{x}) n_{i'} \partial_{i'} G_0^*(\mathbf{x}_1, \mathbf{x}') \} dS' \right] G_0^*(\mathbf{x}_1, \mathbf{x}) \right. \\
 & \left. - \left[\int_{S'} \{ G_0^*(\mathbf{x}_1, \mathbf{x}') n_{i'} \partial_{i'} G_S(\mathbf{x}', \mathbf{x}) \right. \right. \\
 & \left. \left. - G_S(\mathbf{x}', \mathbf{x}) n_{i'} \partial_{i'} G_0^*(\mathbf{x}_1, \mathbf{x}') \} dS' \right] n_{i'} \partial_{i'} G_0^*(\mathbf{x}_1, \mathbf{x}) \right\} dS, \quad (12)
 \end{aligned}$$

where \mathbf{x}_1 is the image point, \mathbf{x} is a source on the boundary S , \mathbf{x}' is a receiver on the boundary S' , and c_0 is the propagation velocity of the homogeneous background medium. In this configuration S and S' coincide, and $G_S(\mathbf{x}', \mathbf{x})$ is the scattered wavefield within the Born approximation (Figure 6). This is an imaging condition that integrates the amount of energy that has been scattered from each location to define the scattering potential at that point, which is a property of the medium (in this formulation, the scattering potential is the difference in the inverse square of the acoustic velocity in the actual medium and the background medium). It does this by performing a dou-

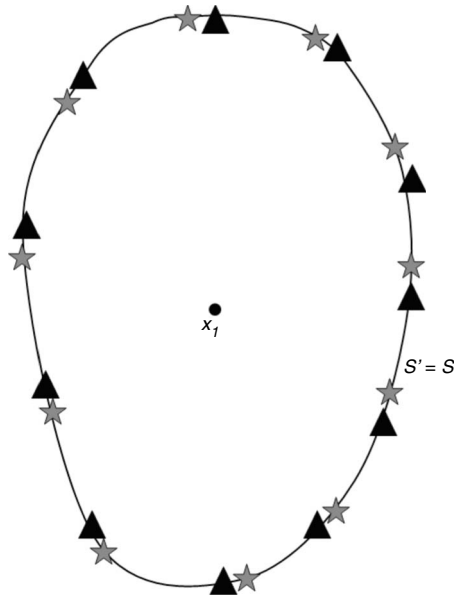


Figure 6. Configuration used by Oristaglio (1989). The scattering potential at a point \mathbf{x}_1 is related to the Green's functions between \mathbf{x}_1 and sources and receivers on a surrounding boundary. Using the same notation as for source-receiver interferometry we see that the boundaries S and S' coincide. S and S' are closed lines in two dimensions, surfaces in three dimensions.

ble focusing at the image point \mathbf{x}_1 : the first focusing step uses the wavefield from the receiver array (\mathbf{x}'), and the second focusing step uses the wavefield from the source array (\mathbf{x}).

We can recognize the double surface integral on the right-hand side as being similar to the source-receiver relation in equation 8 with $\mathbf{x}_1 = \mathbf{x}_2$. Whereas in an application of seismic interferometry all Green's function terms on the right-hand side of equation 8 are directly measured, equation 12 uses measured scattered Green's functions between boundary locations (the terms $G_S(\mathbf{x}', \mathbf{x})$) and modeled background wavefields between the boundaries and the point \mathbf{x}_1 [the terms $G_0(\mathbf{x}_1, \mathbf{x})$ and $G_0(\mathbf{x}_1, \mathbf{x}')$]. Hence, we would expect this integral to give a result similar to the zero offset Green's function. However, Oristaglio's formula explicitly reconstructs the scattering potential within the Born approximation. Hence, the additional frequency-dependent terms on the right-hand side of equation 12 can be considered as a filter, relating the zero-offset Green's function to the scattering potential.

To find the precise link between equations 8 and 12, we set $\mathbf{x}_1 = \mathbf{x}_2$ in equation 8, use source-receiver reciprocity such that all terms on the right-hand side are consistent with equation 12 and obtain

$$\begin{aligned}
 G_S(\mathbf{x}_1, \mathbf{x}_1) - j\omega \int_V (\kappa_0 - \kappa) G(\mathbf{x}, \mathbf{x}_1) G_0^*(\mathbf{x}, \mathbf{x}_1) dV \\
 - \frac{-1}{j\omega\rho} \int_S \left\{ n_i \partial_i \left[j\omega \int_{V'} (\kappa'_0 - \kappa') G(\mathbf{x}', \mathbf{x}) \right. \right. \\
 \left. \left. \times G_0^*(\mathbf{x}', \mathbf{x}_1) dV' \right] G_0^*(\mathbf{x}, \mathbf{x}_1) \right. \\
 \left. - \left[j\omega \int_{V'} (\kappa'_0 - \kappa') G(\mathbf{x}', \mathbf{x}) G_0^*(\mathbf{x}', \mathbf{x}_1) dV' \right] \right. \\
 \left. \times n_i \partial_i G_0^*(\mathbf{x}, \mathbf{x}_1) \right\} dS \\
 = \frac{-1}{j\omega\rho} \int_S \left\{ n_i \partial_i \left[\frac{-1}{j\omega\rho} \int_{S'} \{ G_0^*(\mathbf{x}_1, \mathbf{x}') n_{i'} \partial_{i'} G_S(\mathbf{x}', \mathbf{x}) \right. \right. \\
 \left. \left. - G_S(\mathbf{x}', \mathbf{x}) n_{i'} \partial_{i'} G_0^*(\mathbf{x}_1, \mathbf{x}') \} dS' \right] G_0^*(\mathbf{x}_1, \mathbf{x}) \right. \\
 \left. - \left[\frac{-1}{j\omega\rho} \int_{S'} \{ G_0^*(\mathbf{x}_1, \mathbf{x}') n_{i'} \partial_{i'} G_S(\mathbf{x}', \mathbf{x}) \right. \right. \\
 \left. \left. - G_S(\mathbf{x}', \mathbf{x}) n_{i'} \partial_{i'} G_0^*(\mathbf{x}_1, \mathbf{x}') \} dS' \right] n_{i'} \partial_{i'} G_0^*(\mathbf{x}_1, \mathbf{x}) \right\} dS. \quad (13)
 \end{aligned}$$

The right-hand side of this equation is very similar to the surface integral on the right-hand side of equation 12. However, although equation 12 defines only the approximate (Born) scattering potential, the above formula defines the full zero-offset scattering response (which in turn is related to the scattering amplitude) exactly.

There appear to be significant differences between equation 13 and equation 12. Most notably the scaling terms on the right-hand side of equation 12 are not present in equation 13, and the volume in-

tegrals on the left side of equation 13 are not apparent on the left of equation 12. Although at first it appears that these extra terms are missing, we now show that these volume terms are implicit in Oristaglio's formula for the scattering potential $f(\mathbf{x}_1)$ under the Born approximation, for the case where surfaces S and S' coincide. Thus, we will demonstrate that equation 12 is in fact consistent with (and is a special case of) the source-receiver interferometric scattering integral in equation 13, and hence, that the interferometric equation 13 is an explicit generalization of the imaging equation 12.

We begin by noting that under the Born approximation the scattered wavefield is given by

$$G_S(\mathbf{x}_2, \mathbf{x}_1) = \frac{1}{j\omega\rho} \int_{V''} G_0(\mathbf{x}_2, \mathbf{x}'') f(\mathbf{x}'') G_0(\mathbf{x}'', \mathbf{x}_1) dV'', \quad (14)$$

where we have used $f(\mathbf{x}) = \rho\omega^2(\kappa(\mathbf{x}) - \kappa_0(\mathbf{x}))$. Here it is understood that equation 14 requires Sommerfield radiation conditions on a surface enclosing the volume V'' (Vasconcelos et al., 2009a). Again using the Born approximation, we now write the left-hand side of equation 13 in terms of this volume integral and rearrange to obtain (for the left side only):

$$\begin{aligned} & \frac{1}{j\omega\rho} \int_{V''} G_0(\mathbf{x}_1, \mathbf{x}'') f(\mathbf{x}'') G_0(\mathbf{x}'', \mathbf{x}_1) dV'' \\ & + \frac{1}{j\omega\rho} \int_V G_0(\mathbf{x}_1, \mathbf{x}) f(\mathbf{x}) G_0^*(\mathbf{x}, \mathbf{x}_1) dV \\ & + \frac{-1}{j\omega\rho} \int_S \left\{ n_i \partial_i \left[\frac{1}{j\omega\rho} \int_{V'} G_0(\mathbf{x}', \mathbf{x}) f(\mathbf{x}') G_0^*(\mathbf{x}', \mathbf{x}_1) dV' \right] \right. \\ & \times G_0^*(\mathbf{x}, \mathbf{x}_1) - \left. \left[\frac{1}{j\omega\rho} \int_{V'} G_0(\mathbf{x}', \mathbf{x}) f(\mathbf{x}') \right. \right. \\ & \left. \left. \times G_0^*(\mathbf{x}', \mathbf{x}_1) dV' \right] n_i \partial_i G_0^*(\mathbf{x}, \mathbf{x}_1) \right\} dS, \quad (15) \end{aligned}$$

where under the Born approximation we have replaced $G(\mathbf{x}', \mathbf{x})$ with $G_0(\mathbf{x}', \mathbf{x})$. We now evaluate the surface integral (i.e., by interchanging the positions of the volume and the surface integral and using a seismic interferometry relation to replace the surface integral with interferometric Green's functions) to give

$$\begin{aligned} & \frac{1}{j\omega\rho} \int_{V''} G_0(\mathbf{x}_1, \mathbf{x}'') f(\mathbf{x}'') G_0(\mathbf{x}'', \mathbf{x}_1) dV'' \\ & + \frac{1}{j\omega\rho} \int_V G_0(\mathbf{x}_1, \mathbf{x}) f(\mathbf{x}) G_0^*(\mathbf{x}, \mathbf{x}_1) dV \\ & + \frac{1}{j\omega\rho} \int_{V'} G_0(\mathbf{x}', \mathbf{x}_1) f(\mathbf{x}') G_0^*(\mathbf{x}', \mathbf{x}_1) dV' \\ & + \frac{1}{j\omega\rho} \int_{V'} G_0^*(\mathbf{x}', \mathbf{x}_1) f(\mathbf{x}') G_0^*(\mathbf{x}', \mathbf{x}_1) dV'. \quad (16) \end{aligned}$$

From equation 14 we can see that, within the Born approximation, the first volume integral is equivalent to the zero-offset scattering response, and the fourth volume integral is equivalent to the time-re-

verse of this response (because frequency domain complex conjugation is equivalent to time reversal). The presence of the time-reverse of the scattering response confirms that the event observed in Figure 5c is indeed the time-reverse of the scattered wave. The second and third volume terms are equivalent to the single-scattered wave where the incident wave has propagated in time reverse. This can be understood by considering that the back-propagated wavefield from an enclosing boundary will have a forward (causal) and reverse (acausal) time part, in the same way that seismic interferometry provides causal and acausal responses (e.g., Wang and Oristaglio, 1998; Thorbecke and Wapenaar, 2007). It is also interesting to note that these second and third terms can be recognized as being similar to the non-physical waves identified in seismic interferometric theory that arise due to scattering (e.g., Snieder et al., 2008; Halliday and Curtis; 2009a, b; Vasconcelos et al., 2009a).

If as in Oristaglio (1989) we now assume that the volumes V'' , V' , and V are the same and further define the homogeneous Green's function as $G_0^h(\mathbf{x}_1, \mathbf{x}'') = G_0(\mathbf{x}_1, \mathbf{x}'') + G_0^*(\mathbf{x}_1, \mathbf{x}'')$, then we find that equation 16 is equal to $1/j\omega\rho \int_V G_0^h(\mathbf{x}_1, \mathbf{x}) f(\mathbf{x}) G_0^h(\mathbf{x}_1, \mathbf{x}) dV$. Hence, equation 13 becomes

$$\begin{aligned} & \frac{1}{j\omega\rho} \int_V G_0^h(\mathbf{x}_1, \mathbf{x}) f(\mathbf{x}) G_0^h(\mathbf{x}_1, \mathbf{x}) dV \\ & = \frac{-1}{j\omega\rho} \int_S \{ n_i \partial_i \Phi(\mathbf{x}_1, \mathbf{x}) G_0^*(\mathbf{x}_1, \mathbf{x}) \\ & \quad - \Phi(\mathbf{x}_1, \mathbf{x}) n_i \partial_i G_0^*(\mathbf{x}_1, \mathbf{x}) \} dS, \quad (17) \end{aligned}$$

where the term in the inner surface integral has been replaced by $\Phi(\mathbf{x}_1, \mathbf{x})$, which is equivalent to the back propagated wavefield at \mathbf{x}_1 (cf. Esmersoy and Oristaglio, 1988, equation 1):

$$\begin{aligned} \Phi(\mathbf{x}_1, \mathbf{x}) & = \frac{-1}{j\omega\rho} \int_{S'} \{ n_{i'} \partial_{i'} G_S(\mathbf{x}', \mathbf{x}) G_0^*(\mathbf{x}_1, \mathbf{x}') \\ & \quad - G_S(\mathbf{x}', \mathbf{x}) n_{i'} \partial_{i'} G_0^*(\mathbf{x}_1, \mathbf{x}') \} dS'. \quad (18) \end{aligned}$$

Note that if we apply the same approximations used in equation 11, the quantity we have defined as $\Phi(\mathbf{x}_1, \mathbf{x})$ can also be considered to be equivalent to the adjoint operator applied in techniques such as acoustic phase conjugation or time reversal (e.g., Kuperman et al., 1998).

Oristaglio (1989) shows that for a homogeneous background medium the time derivative of the homogeneous Green's function, evaluated at time zero, yields a spatial delta function. He uses this property of the homogeneous Green's function to show that, within the Born approximation, the scattering amplitude is equivalent to

$$\begin{aligned} f(\mathbf{x}_1) & = \left(\frac{4}{jc_0} \int_{-\infty}^{\infty} d\omega (-i\omega) \frac{\partial}{\partial \omega} \right) \\ & \quad \times \int_V G_0^h(\mathbf{x}_1, \mathbf{x}) f(\mathbf{x}) G_0^h(\mathbf{x}_1, \mathbf{x}) dV. \quad (19) \end{aligned}$$

Comparing the left-hand side of equation 17 with the right-hand side of equation 19, it is clear that the volume terms are required in order to derive Oristaglio's formula for the scattering amplitude. Hence, although no volume integrals appear in equation 12 from Oristaglio (1989), equation 19 shows that his formula for the scattering ampli-

tude is consistent with the theory of source to receiver scattering defined by source-receiver interferometry.

By applying the operator in brackets in equation 19 to both sides of equation 18 we finally obtain

$$f(\mathbf{x}_1) = \frac{-4}{jc_0} \int_{-\infty}^{\infty} d\omega(-j\omega) \frac{\partial}{\partial \omega} \times \int_S \{n_i \partial_i \Phi(\mathbf{x}_1, \mathbf{x}) G_0^*(\mathbf{x}_1, \mathbf{x}) - \Phi(\mathbf{x}_1, \mathbf{x}) n_i \partial_i G_0^*(\mathbf{x}_1, \mathbf{x})\} dS. \quad (20)$$

Recalling our definition of $\Phi(\mathbf{x}_1, \mathbf{x})$ in equation 18, we can see that equation 20 is nearly identical to equation 12. Therefore, by applying the conditions set by Oristaglio (single-scattering Born approximation and homogeneous background medium, $V = V'$, and $S = S'$) to the source-receiver interferometric scattering representation in equation 8, we have shown an explicit link between source-receiver interferometry and seismic imaging theory. Note the slight differences between equation 20 and equation 12: these additional terms are due to the choice of Green's functions and definition of the scattering amplitude used here, but do not affect the result.

The inclusion of the volume terms in equation 16 in the formula for $f(\mathbf{x}_1)$ in equation 19 indicates that these are implicit in Oristaglio's earlier derivation. When applying seismic interferometry to perturbed wavefields these terms are treated as nonphysical, because they do not correspond to part of the interreceiver (or in this case, source-receiver) wavefield and may indeed be treated as a source of error. However, here we have shown that these terms are crucial in deriving Oristaglio's imaging condition.

DISCUSSION

The derivation of Oristaglio's imaging condition from the new source-receiver representation creates an explicit link between this new form of seismic interferometry and inverse-scattering imaging theory. It is interesting to note that in 1989 Oristaglio derived what may be considered an interferometric integral, and indeed he also derived an integral similar to the source-receiver form derived here, albeit for a more limited geometry. Integral equations describing extrapolated wavefields can readily be identified as being of the same form as interferometric integrals (e.g., Schneider, 1978; Esmersoy and Oristaglio, 1988). Hence, although interferometry provides a new approach to seismic data analysis, much of the theoretical

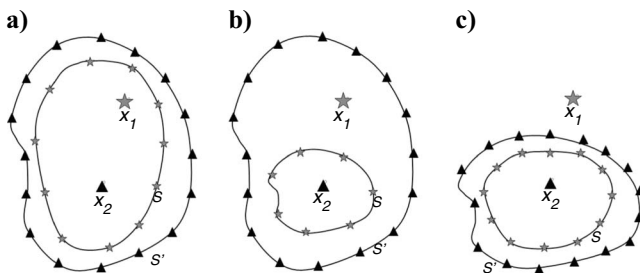


Figure 7. Canonical geometries. Triangles represent receivers; stars represent sources. S and S' are closed lines in two dimensions and surfaces in three dimensions. (a) Configuration considered in this manuscript, where equation 1 and 2 are both correlation-type reciprocity theorems, (b) configuration where equation 1 and 2 are correlation- and convolution-type reciprocity theorems respectively, and (c) configuration where equation 1 and 2 are convolution-type reciprocity theorems.

framework for seismic interferometry has been used for imaging for several decades [see Thorbecke and Wapenaar (2007) for further discussion].

Oristaglio's derivation of equation 12 relies on a single-scattering approximation. Note that the process used to reach equation 16 from equation 13 may be iterated to account for multiple scattering. However, it is unlikely in this case that the result will be as elegant as the case derived by Oristaglio. Iteration of the process would require the volume terms in equation 10 to be included and would also require the full scattered field to be included in the other volume integrals. However, this may be a useful way to quantify the effect of including scattering beyond the Born approximation in imaging and migration.

We have shown that Oristaglio's imaging equation 12 is a particular case of our new interferometric equation 8. It was not previously possible to make the link between imaging and interferometry explicit because previous interferometric relations used only a single boundary of sources or of receivers, whereas imaging is usually done using both boundaries of sources and of receivers. Unlike equation 12, equation 8 was derived without using the Born approximation and without the requirement that the boundaries of sources and receivers coincide. Hence, the interferometric equation 8 can be thought of as a generalized imaging equation, such as that used by Vasconcelos et al. (2009b).

Equations similar to equation 8 are currently being used to create so-called "extended images" via image-domain interferometry in seismic migration (e.g., Vasconcelos et al., 2009b; Sava and Vasconcelos, 2009). These extended images provide a tool to analyze the quality of migrated seismic data, and can be used to refine velocity models. The extended images are treated as scattered wavefields, arising from virtual sources created within the seismic image. The equations used by Vasconcelos et al. (2009b) assume that the scattered wavefield has already been back-propagated from the receivers, into the subsurface. This results in some of the volume terms in equation 8 not being explicit. If such volume terms are ignored by practitioners, they may result in error. In the case of one set of volume terms, Vasconcelos et al. (2009b) suggest that they can be used to deal with sharp boundaries in the background model. Presumably accounting for both sets of volume terms in equation 8 would further improve results in the sharp-boundary scenario. Further analysis of the volume terms appearing in equation 8 may allow for better understanding of the role of these terms and what, if any, new information they can provide.

Although we have derived this imaging equation using two correlational reciprocity theorems, it is also possible to derive expressions such as equation 8 using a correlational and a convolutional reciprocity relation and also using two convolutional relations [see Curtis and Halliday (2010b) for details]. These different approaches allow for many different source and receiver geometries to be analyzed [the three canonical geometries of Curtis and Halliday (2010b) are illustrated in Figure 7 for various combinations of correlation and convolution]. Also, there are several different reciprocity theorems for perturbed media, meaning that there are many more combinations of reciprocity theorems that could be used in this case (Vasconcelos et al., 2009a). Hence, although we have considered one case and shown the link between source-receiver interferometry and seismic imaging, there are many other forms that can be derived similarly, and these may allow for the development of new imaging conditions or new applications of source-receiver interferometry to seismic data.

Finally, it is also possible to derive source-receiver scattering relationships for other wave propagation regimes, including elastic wave propagation (van Manen et al., 2006, Wapenaar and Fokkema, 2006), electromagnetic wavefields (Slob and Wapenaar, 2007; Slob et al., 2007), and seismo-electric wave propagation and diffusion phenomena (Wapenaar et al., 2006; Snieder et al., 2007; Vasconcelos, 2008). We therefore expect the derivation of similar explicit relationships between imaging and interferometry to become tractable in those regimes also.

CONCLUSIONS

In this paper, we have shown how the source-receiver interferometry approach can be extended to the case of perturbed media by using reciprocity theorems for scattered wavefields. We derived one of a new class of interferometric integrals that describe the recovery of scattered wavefields propagating between source and receiver locations.

The new scattering relationship has been illustrated using a simple acoustic example. This example utilized the far-field approximation, commonly used when deriving interferometric relations for passive (background noise) wavefields. Hence the new source-receiver scattering theorems show how both energy from passive noise and active sources can be combined to create a subsurface image.

Rather than focusing on applications of these new source-receiver relations, we have shown that existing imaging conditions can be derived directly from the new interferometric representation. Although this requires that the scattering be constrained by the Born approximation and that the bounding surfaces of sources and receivers coincide, it creates an explicit link between source-receiver interferometric representations and inverse-scattering seismic imaging.

ACKNOWLEDGMENTS

The authors thank Deyan Draganov, Jan Thorbecke, and an anonymous reviewer for their invaluable comments that helped to improve the manuscript. We also thank Ivan Vasconcelos for his encouragement and suggestions.

REFERENCES

- Berkhout, A. J., 1997, Pushing the limits of seismic imaging, part I: Prestack migration in terms of double dynamic focusing: *Geophysics*, **62**, 937–953.
- Curtis, A., and D. Halliday, 2010a, Directional balancing for seismic and general wavefield interferometry: *Geophysics*, **75**, no. 1, SA1–SA14.
- Curtis, A., and D. Halliday, 2010b, Source-receiver wavefield interferometry: *Physical Review E: Statistical, Nonlinear, and Soft Matter Physics*, **81**, no. 4, 046601.
- Curtis, A., H. Nicolson, D. Halliday, J. Trampert, and B. Baptie, 2009, Chicken and egg: Turning earthquakes into subsurface seismic sensors: *Nature Geoscience*, **NGEO615**, **2**, 700–704.
- Curtis, A., P. Gerstoft, H. Sato, R. Snieder, and K. Wapenaar, 2006, Seismic interferometry — Turning noise into signal: *The Leading Edge*, **25**, 1082–1092.
- Derode, A., E. Larose, M. Campillo, and M. Fink, 2003, How to estimate the Green's function of a heterogeneous medium between two passive sensors? Application to acoustic waves: *Applied Physics Letters*, **83**, no. 15, 3054–3056.
- Esmeroy, C., and M. Oristaglio, 1988, Reverse-time wave-field extrapolation, imaging, and inversion: *Geophysics*, **53**, 920–931.
- Fokkema, J. T., and P. M. van den Berg, 1993, *Seismic applications of acoustic reciprocity*, Elsevier.
- Groenenboom, J., and R. Snieder, 1995, Attenuation, dispersion and anisotropy by multiple scattering of transmitted waves through distributions of scatterers: *The Journal of the Acoustical Society of America*, **98**, no. 6, 3482–3492.
- Halliday, D., and A. Curtis, 2009a, Generalized optical theorem for surface waves and layered media: *Physical Review E: Statistical, Nonlinear, and Soft Matter Physics*, **79**, no. 5, 056603.
- Halliday, D., and A. Curtis, 2009b, Seismic interferometry of scattered surface waves in attenuative media: *Geophysical Journal International*, **178**, no. 1, 419–446.
- Halliday, D., A. Curtis, P. Vermeer, C. Strobbia, A. Glushchenko, D.-J. van Manen, and J. O. A. Robertsson, 2010, Interferometric ground-roll removal: Attenuation of scattered surface waves from single-sensor data: *Geophysics*, **75**, no. 2, SA15–SA25.
- Kuperman, W. A., W. S. Hodgkiss, and H. C. Song, 1998, Phase conjugation in the ocean: Experimental demonstration of an acoustic time-reversal mirror: *The Journal of the Acoustical Society of America*, **103**, no. 1, 25–40.
- Oristaglio, M. L., 1989, An inverse-scattering formula that uses all the data: *Inverse Problems*, **5**, no. 6, 1097–1105.
- Sava, P., and I. R. Vasconcelos, 2009, Efficient computation of extended images by wavefield-based migration: 79th Annual International Meeting, SEG, Expanded Abstracts, 2824–2828.
- Schneider, W. A., 1978, Integral formulation for migration in two and three dimensions: *Geophysics*, **43**, 49–76.
- Schuster, G. T., and J. Hu, 2000, Green's function for migration: Continuous recording geometry: *Geophysics*, **65**, 167–175.
- Slob, E., and K. Wapenaar, 2007, Electromagnetic Green's functions retrieval by cross-correlation and cross-convolution in media with losses: *Geophysical Research Letters*, **34**, no. 5, L05307.
- Slob, E., D. Draganov, and K. Wapenaar, 2007, Interferometric electromagnetic Green's functions representations using propagation invariants: *Geophysical Journal International*, **169**, no. 1, 60–80.
- Snieder, R., K. van Wijk, M. Haney, and R. Calvert, 2008, Cancellation of spurious arrivals in Green's function extraction and the generalized optical theorem: *Physical Review E: Statistical, Nonlinear, and Soft Matter Physics*, **78**, no. 3, 036606.
- Snieder, R., K. Wapenaar, and U. Wegler, 2007, Unified Green's function retrieval by cross-correlation; connection with energy principles: *Physical Review E: Statistical, Nonlinear, and Soft Matter Physics*, **75**, no. 3, 036103.
- Thorbecke, J., and K. Wapenaar, 2007, On the relation between seismic interferometry and the migration resolution function: *Geophysics*, **72**, no. 6, T61–T66.
- van Manen, D.-J., J. O. A. Robertsson, and A. Curtis, 2005, Modeling of wave propagation in inhomogeneous media: *Physical Review Letters*, **94**, no. 16, 164301.
- van Manen, D.-J., A. Curtis, and J. O. A. Robertsson, 2006, Interferometric modeling of wave propagation in inhomogeneous elastic media using time reversal and reciprocity: *Geophysics*, **71**, no. 4, S147–S160.
- Vasconcelos, I., and R. Snieder, 2008a, Interferometry by deconvolution, Part 1 — Theory for acoustic waves and numerical examples: *Geophysics*, **73**, no. 3, S115–S128.
- Vasconcelos, I., and R. Snieder, 2008b, Interferometry by deconvolution: Part 2 — Theory for elastic waves and application to drill-bit seismic imaging: *Geophysics*, **73**, no. 3, S129–S141.
- Vasconcelos, I., 2008, Generalized representations of perturbed fields — Applications in seismic interferometry and migration, 78th Annual International Meeting, SEG, Expanded Abstracts, 2927–2931.
- Vasconcelos, I. R., R. Snieder, and H. Douma, 2009a, Representation theorems and Green's function retrieval for scattering in acoustic media: *Physical Review E: Statistical, Nonlinear, and Soft Matter Physics*, **80**, no. 3, 036605.
- Vasconcelos, I. R., P. Sava, and H. Douma, 2009b, Wave-equation extended images via image-domain interferometry, 79th Annual International Meeting, SEG, Expanded Abstracts, 2839–2843.
- Wang, T., and M. L. Oristaglio, 1998, An inverse algorithm for velocity reconstruction: *Inverse Problems*, **14**, no. 5, 1345–1351.
- Wapenaar, K., 2003, Synthesis of an inhomogeneous medium from its acoustic transmission response: *Geophysics*, **68**, 1756–1759.
- Wapenaar, K., 2004, Retrieving the elastodynamic Green's function of an arbitrary inhomogeneous medium by cross correlation: *Physical Review Letters*, **93**, no. 25, 254301.
- Wapenaar, K., 2007, General representations for wavefield modeling and inversion in geophysics: *Geophysics*, **72**, no. 5, SM5–SM17.
- Wapenaar, K., D. Draganov, and J. O. A. Robertsson, eds., 2008a, *Seismic interferometry: History and present status*: SEG Geophysics Reprint Series No. 26.
- Wapenaar, K., E. Slob, and R. Snieder, 2006, Unified Green's function retrieval by cross correlation: *Physical Review Letters*, **97**, no. 23, 234301.
- Wapenaar, K., E. Slob, and R. Snieder, 2008b, Seismic and electromagnetic controlled-source interferometry in dissipative media: *Geophysical Prospecting*, **56**, no. 3, 419–434.
- Wapenaar, K., and J. Fokkema, 2006, Green's function representations for seismic interferometry: *Geophysics*, **71**, no. 4, S133–S144.